--- Supporting Information ---

Structural Insights into Bound Water in Crystalline Amino Acids: Experimental and Theoretical ^{17}O NMR

Vladimir K. Michaelis[1*], Eric G. Keeler[1], Ta-Chung Ong[1‡], Kimberley N. Craigen[2], Susanne Penzel[1†], John E. C. Wren[2], Scott Kroeker[2*] and Robert G. Griffin[1*]

1-Department of Chemistry and Francis Bitter Magnet Laboratory, Massachusetts Institute of Technology, Cambridge, Massachusetts, 02139 USA

2-Department of Chemistry, University of Manitoba, Winnipeg, Manitoba, R3T 2N2 Canada

‡-Current Address: Department of Chemistry, Laboratory of Inorganic Chemistry, ETH- Zürich, CH-8093 Zürich, Switzerland

†-Current Address: Department of Chemistry and Applied Biosciences, Laboratory of Physical Chemistry, ETH-Zürich, CH-8093 Zürich, Switzerland

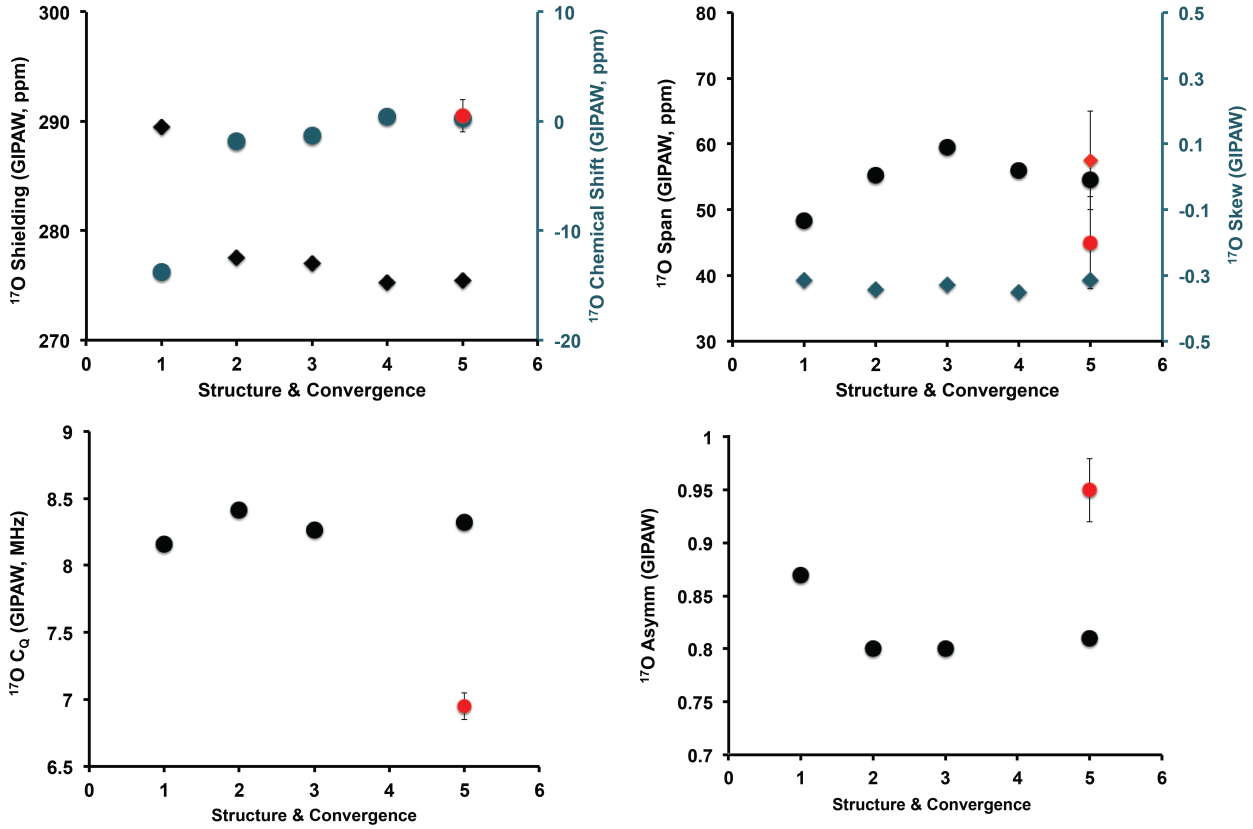

Figure S1: Asn neutron crystal structure using various treatments to test GIPAW convergence criteria. (1) neutron structure (med), (2) H-optimized structure at medium, (3) H-optimized structure at fine, (4) H-optimized structure at ultrafine and (5) all-atom optimization at fine. Red data points are experimental data.

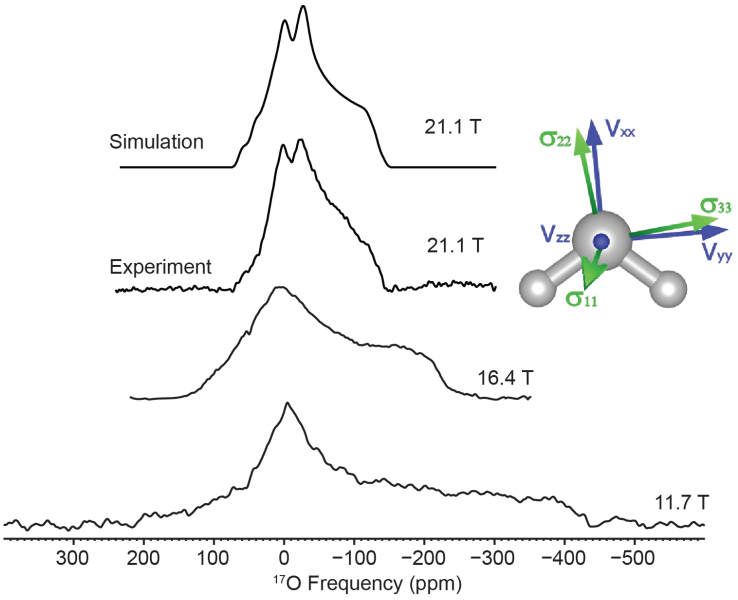

Figure S2: ^{17}O non-spinning NMR spectra of sodium L-aspartic acid monohydrate with ^{1}H decoupling at 11.7, 16.4, and 21.1 T. Simulation of the data: C_Q = 6.9 MHz, η = 0.92, δ_{iso} = -4 ppm, Ω = 50 ppm, κ = 0.9

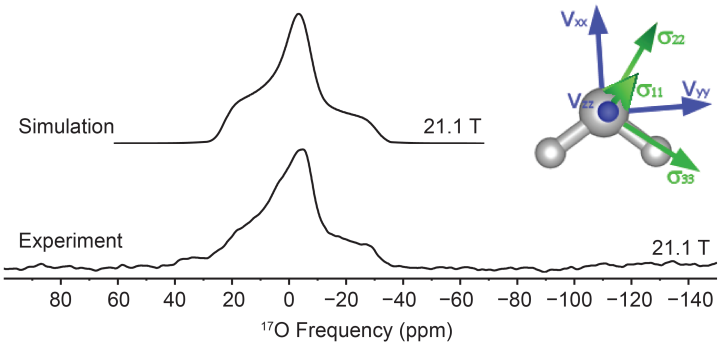

Figure S3: ^{17}O MAS NMR (21 .1 T) of L-arginine•HCl•H_2O at 21.1 T. Simulation parameters: C_Q = 7.0 MHz, η = 0.88, δ_{iso} = 26 ppm.

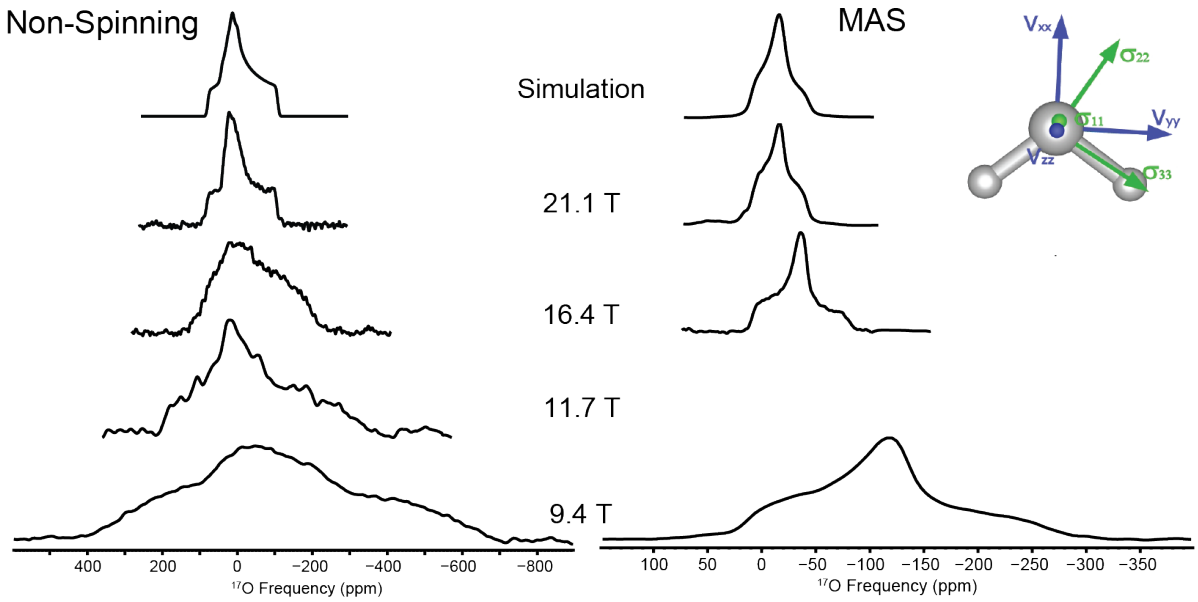

Figure S4: ^{17}O non-spinning (left) and MAS (right) NMR of L-histidine•HCl•H_2O at 9.4, 11.7, 16.4, and 21.1 T. Simulation of the non-spinning data: C_Q = 7.1 MHz, η = 0.95, δ_{iso} = 14 ppm, Ω = 45 ppm, κ = 0.5. Simulation of the MAS data: C_Q = 7.1 MHz, η = 0.95, δ_{iso} = 14 ppm.

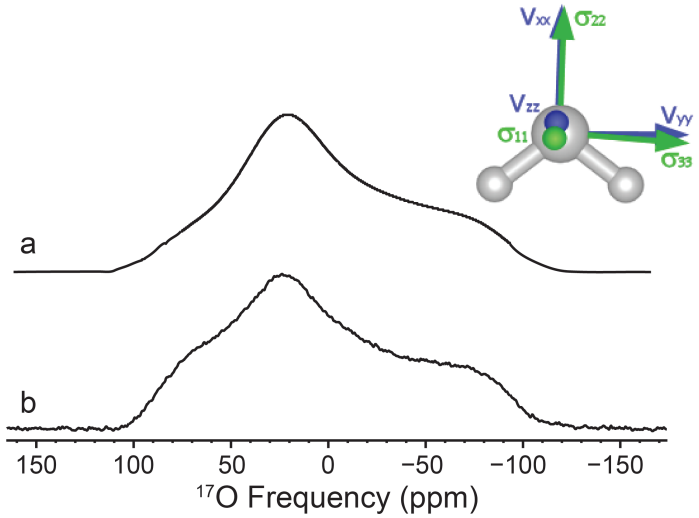

Figure S5: ^{17}O non-spinning NMR spectrum of L-cysteine•HCl•H_2O – (a) Simulation, C_Q = 7.0 MHz, η = 0.90, δ_{iso} = 31 ppm, Ω = 40 ppm and κ = 0.6 and (b) experimental at 21.1 T.

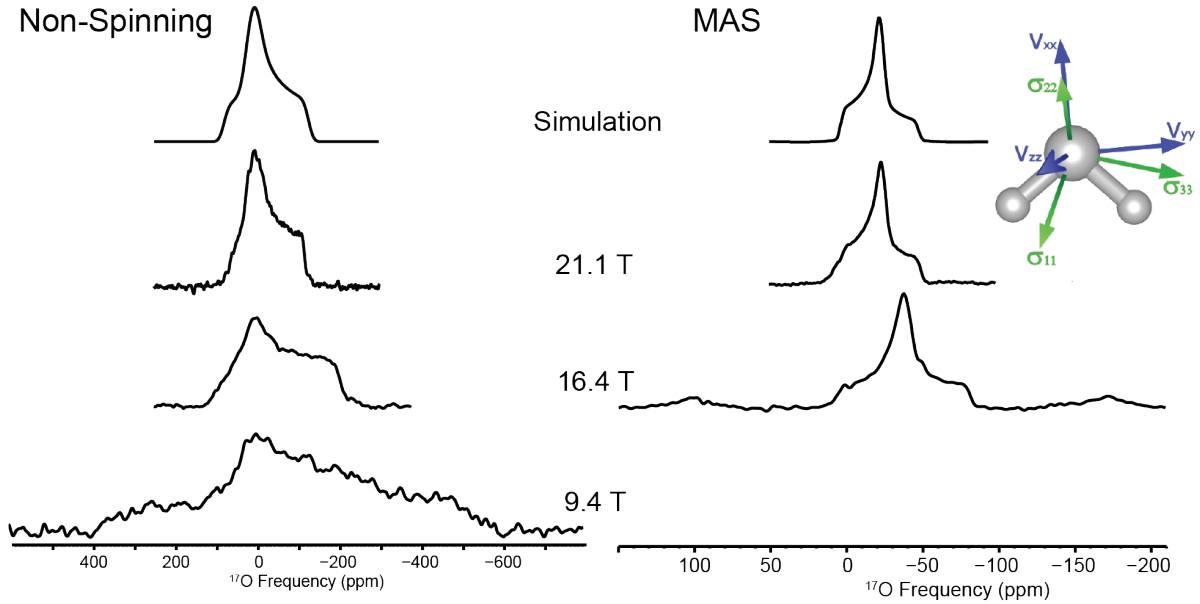

Figure S6: ^{17}O non-spinning (left) and MAS (right) NMR of L-glycylglutamine•H_2O at 9.4, 16.4, and 21.1 T. Simulation of the non-spinning data: C_Q = 7.1 MHz, η = 0.95, δ_{iso} = 8.5 ppm, Ω = 40 ppm, κ = -0.4. Simulation of the MAS data: C_Q = 7.1 MHz, η = 0.95, δ_{iso} = 8.5 ppm.

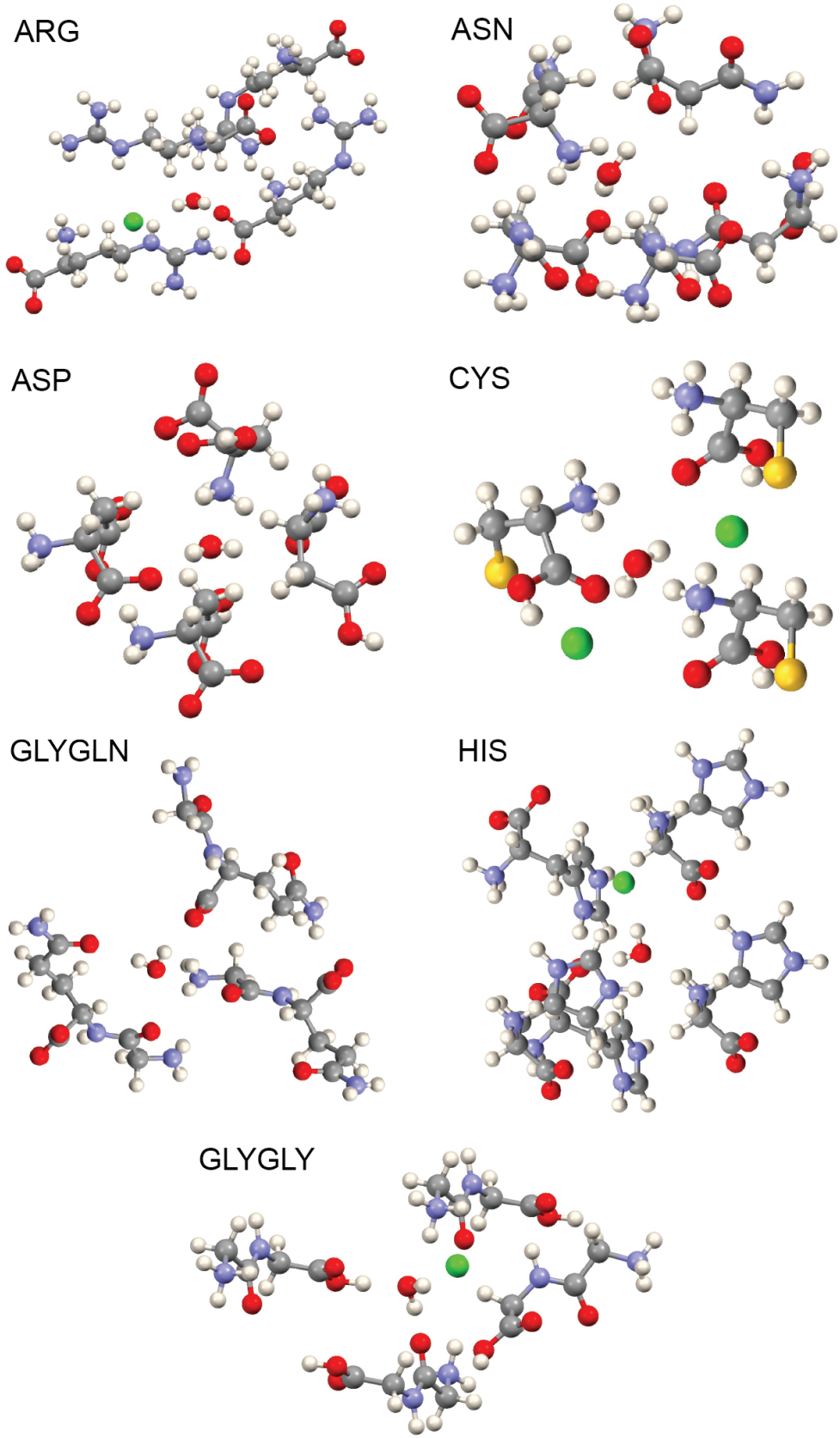

Figure S7: Extended cluster models used within the hybrid-DFT study. Atom designations are as follows: H (white), C (grey), O (red), N (lavender), Cl (green) and S (yellow).

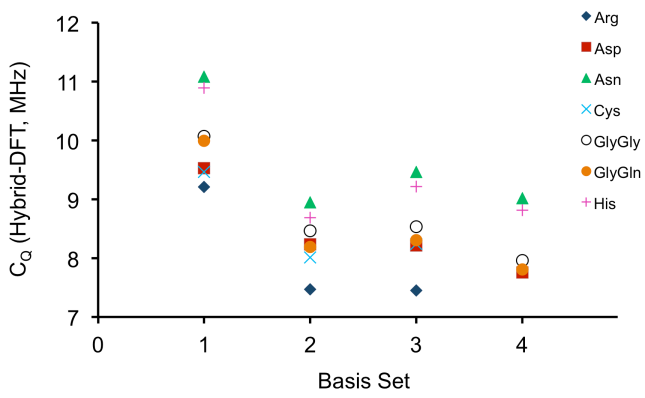

Figure S8: Hybrid-DFT crystal structure convergence for single molecular unit without all atom optimization: (1) 6-31, (2)-6-321+G(d), (3) 6-3211++G(d,p) and (4) aug-cc-pvtz.

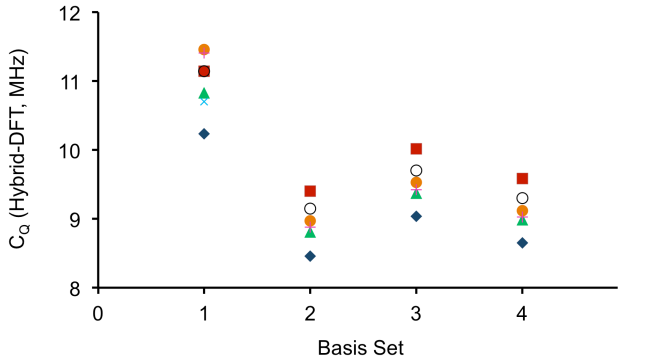

Figure S9: Hybrid-DFT crystal structure convergence for single molecular unit with all atom optimization: (1) 6-31, (2)-6-311+G(d), (3) 6-311++G(d,p) and (4) aug-cc-pvtz.

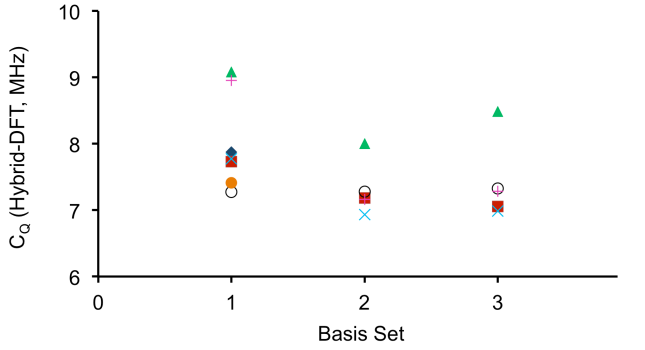

Figure S10: Hybrid-DFT crystal structure convergence for extended structures: (1) 6-31, (2)-6-311+G(d), and (3) 6-311++G(d,p).

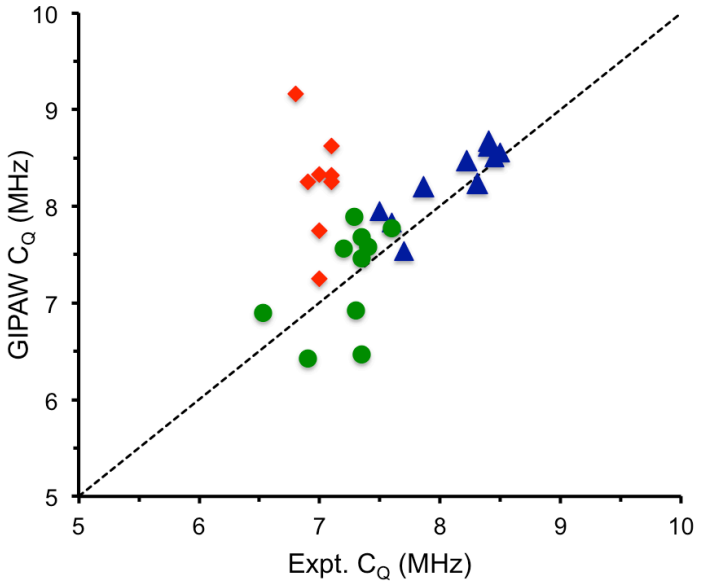

Figure S11: ^{17}O experimental and calculated (GIPAW) quadrupolar coupling constants for C=*O* (blue, triangle), CO*O*H (green, circle) and H_2O (red, diamond) for various amino acid crystalline structures.[1-4]

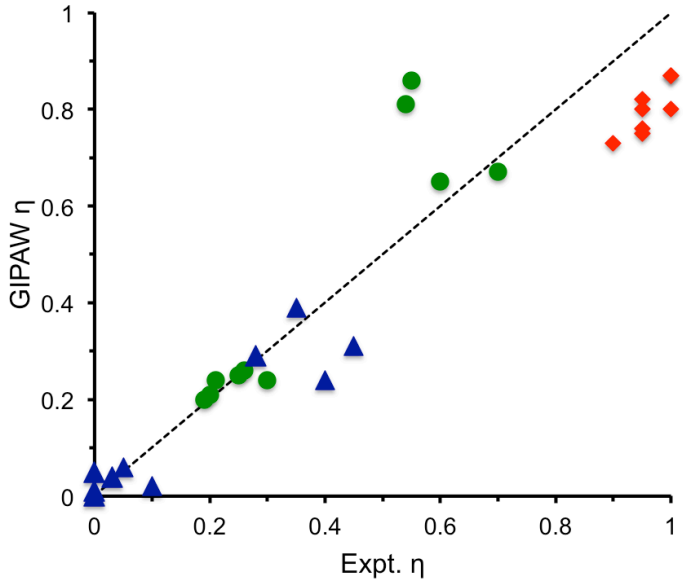

-

Figure S12: ^{17}O experimental and calculated (GIPAW) quadrupolar asymmetry parameters for C=*O* (blue, triangle), CO*O*H (green, circle) and H_2O (red, diamond) for various amino acid crystalline structures.[1-4]

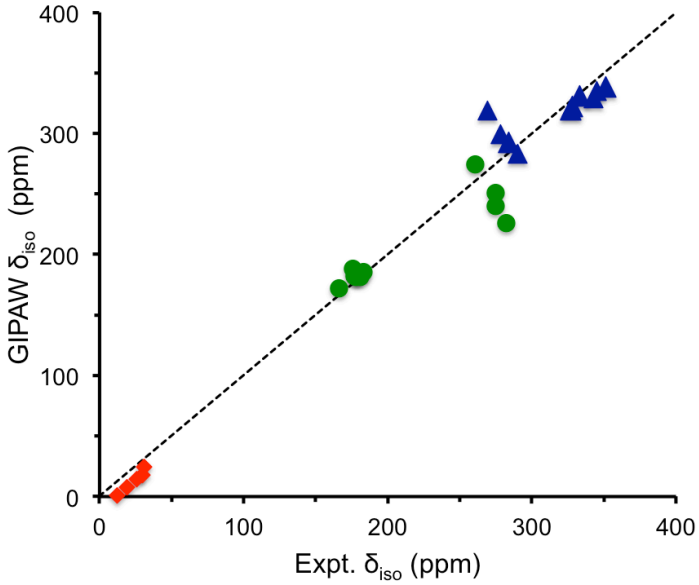

Figure S13: ^{17}O experimental and calculated (GIPAW) isotropic chemical shifts for C=*O* (blue, triangle), CO*O*H (green, circle) and H_2O (red, diamond) for various amino acid crystalline structures.[1-4]

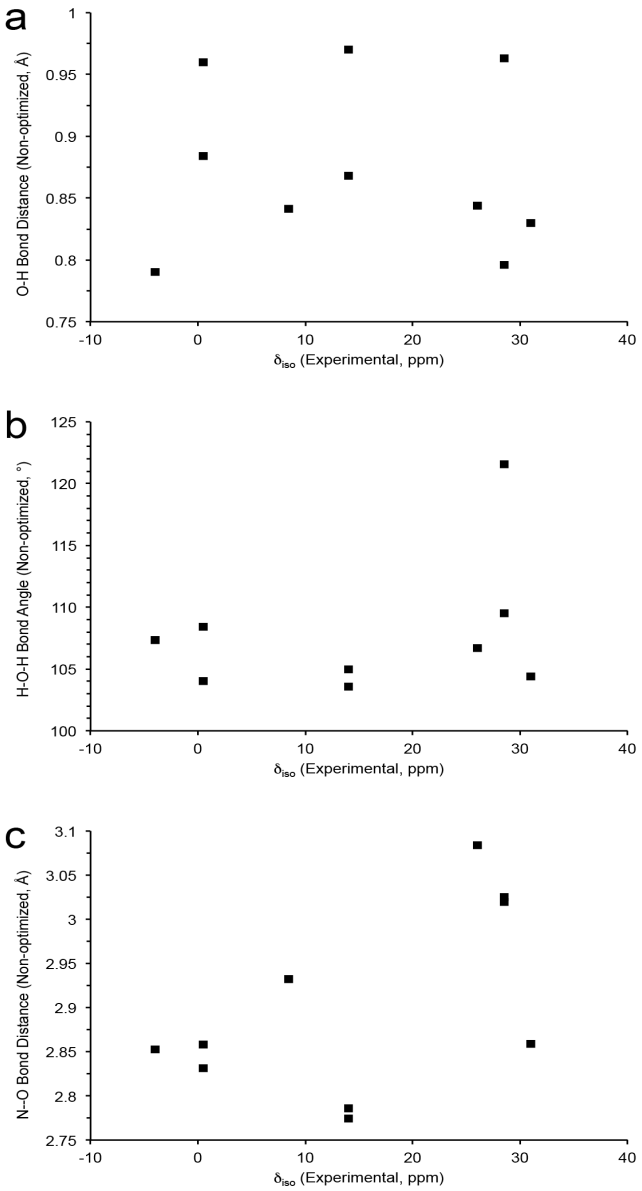

Figure S14: Relationship between ^{17}O NMR chemical shift (ppm) and (a) O-H bond distance from x-ray and neutron structures, (b) H-O-H bond angle from x-ray and neutron structures, and (c) H_2O---NH_3 distance from x-ray and neutron structures.

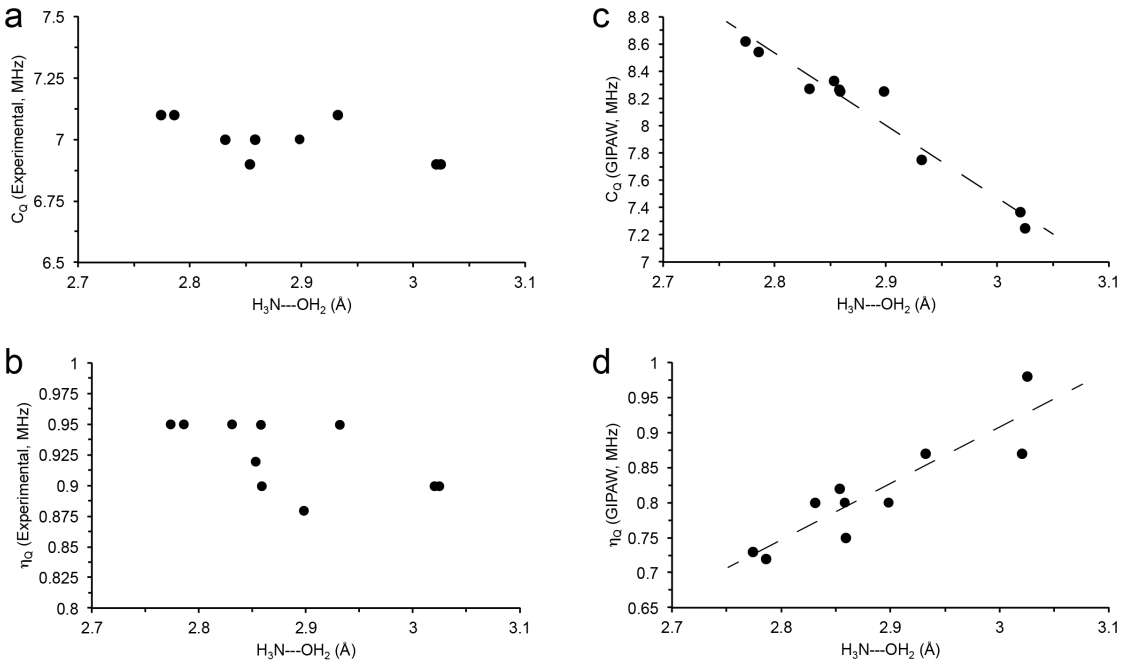

Figure S15: The relationship between: (a) experimental ^{17}O quadrupolar coupling constant, (b) experimental ^{17}O quadrupolar asymmetry parameter, (c) GIPAW calculated ^{17}O quadrupolar coupling constant, (d) GIPAW calculated ^{17}O quadrupolar asymmetry parameter and the hydrogen bond distance between the amine functional group and water molecule (*i.e.,* H_3N---OH_2) from crystalline data.

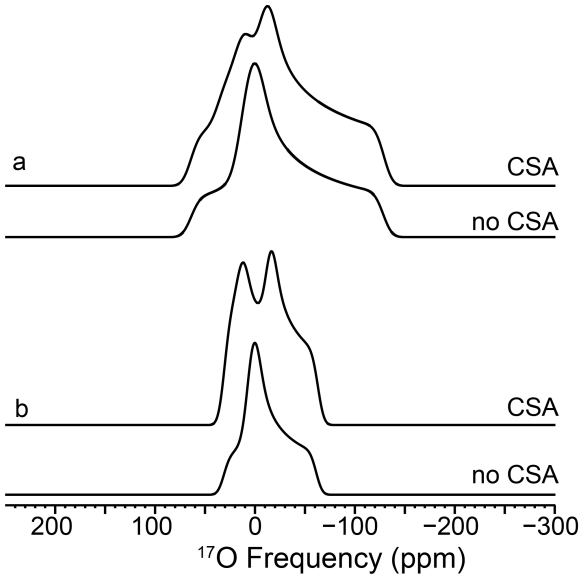

Figure S16: Simulated ^{17}O non-spinning NMR of Asn using parameters measured in this work: (a) at 21.1 T (900 MHz ^{1}H) with (above) and without (below) the CSA included and (b) at 30.5 T (1,300 MHz ^{1}H) with (above) and without (below) the CSA included.

Table S1: ^{17}O GIPAW calculated parameters for neutron and x-ray structures using H-optimized structures

Sample	Oxygen site	C_Q (MHz)	η	σ_{iso} (ppm)	Ω (ppm)	κ	σ_{11} (ppm)	σ_{22} (ppm)	σ_{33} (ppm)
Asn^N	H_2O	8.267	0.8	277.04	59.544	-0.333	310.12	270.424	250.576
	OH	6.924	0.65	22.75	372.708	-0.361	231.55	-22.142	-141.158
	CO	7.537	0.39	-20.89	453.228	-0.399	235.897	-81.235	-217.332
	CON	8.047	0.41	-15.57	524.07	-0.499	290.01	-102.66	-234.06
Asp^N	H_2O	8.326	0.82	275.42	53.868	-0.333	305.347	269.435	251.479
	CO	7.835	0.31	-56.13	487.363	-0.429	222.363	-125.753	-265
	CO	8.695	0.18	-86.32	528.614	-0.54	225.547	-181.439	-303.067
	OH	6.426	0.81	36.58	329.505	-0.27	216.147	6.952	-113.358
	OH	-8.187	0.13	71.12	255.632	0.922	159.672	149.648	-95.96
Arg^X	H_2O	8.254	0.82	248.51	55.895	-0.324	279.476	242.473	223.581
	H_2O	8.248	0.78	247.14	54.648	-0.636	280.26	235.548	225.612
	OH	7.44	0.44	5.43	396.109	-0.343	226.103	-39.808	-170.005
	OH	6.547	0.73	-0.62	367.76	-0.371	205.987	-46.073	-161.773
	CO	7.331	0.4	-34.39	401.141	-0.468	197.483	-96.996	-203.658
	CO	8.178	0.25	-18.51	478.409	-0.438	255.65	-88.421	-222.759
Cys^X	H_2O	8.252	0.75	237.71	39.784	-0.279	259.45	234.014	219.666
	OH	-7.559	0.26	74.48	258.482	0.785	169.882	142.158	-88.6
	CO	8.508	0.06	-72.79	599.8	-0.509	277.97	-174.51	-321.83
His^N	H_2O	8.62	0.73	261.45	49.961	0.306	283.884	266.542	233.923
	OH	6.475	0.85	10.81	365.878	-0.117	200.877	-3.445	-165.002
	CO	8.033	0.27	-41.41	509.807	-0.39	246.617	-107.656	-263.191
His^X	H_2O	8.544	0.72	260.89	50.592	0.235	284.209	264.845	233.617
	OH	6.468	0.86	11.76	366.088	-0.085	199.98	1.408	-166.108
	CO	7.951	0.24	-36.69	509.477	-0.39	251.15	-102.893	-258.327
GlyGly^N	H_2O	7.248	0.93	260.25	49.657	-0.478	289.037	252.334	239.38
	OH	-7.582	0.25	97.63	241.001	0.947	180.078	173.736	-60.923
	CO	8.558	0.05	-65.72	588.503	-0.55	282.507	-173.67	-305.996
	CCOC	7.954	0.42	-8.04	594.111	-0.509	339.393	-108.796	-254.718
GlyGly^X	H_2O	7.367	0.87	245.03	53.68	-0.604	277.27	234.23	233.59
	OH	-7.549	0.24	90.36	244.051	0.947	173.851	167.429	-70.2
	CO	8.553	0.02	-66.62	582.602	-0.571	280.167	-177.592	-302.435
	CCOC	7.86	0.42	-4.45	584.831	-0.509	337.557	-103.632	-247.275
GlyGln^X	H_2O	7.748	0.87	268.62	50.321	-0.448	297.54	261.101	247.219
	CO	8.422	0.23	-53.1	454.291	-0.343	199.987	-104.983	-254.304
	OH	7.164	0.66	13.56	364.174	-0.235	209.88	-14.906	-154.294
	CON	8.183	0.32	-2.33	611.044	-0.458	349.857	-95.659	-261.187
	CON	8.702	0.34	-20.71	568.38	-0.488	309.743	-113.237	-258.636
Ice^N	H_2O	-6.632	0.91	324.57	34.419	-0.529	344.817	318.496	310.397
	H_2O	-7.034	0.88	319.25	36.761	-0.27	339.283	315.944	302.522

^{X} – x-ray determined crystal structure and ^{N} – neutron determined crystal structure.

Table S2: Crystalline and GIPAW-optimized structural data for crystalline amino acid monohydrates

Compound	H-O†* distance (Å)	<HOH† (angle)	N---O† distance (Å)	H-O‡* distance (Å)	<HOH‡ (angle)	N---O‡ distance (Å)
Arg	0.895	103.65	2.898	0.989	104.92	2.898
Asp	0.790	107.34	2.853	0.988	107.38	2.853
Asn	0.960	108.11	2.858	0.987	107.22	2.858
Cys	0.830	104.42	2.877	0.992	105.46	2.877
His	0.972	104.86	2.774	0.990	105.51	2.774
Gly-Gly	0.963	109.52	3.025	0.996	108.51	3.020
Gly-Gln	0.840	97.72	3.309	0.990	105.31	3.309

† - Crystal structural parameters
‡ - GIPAW optimized structural parameters
* - Average H-O bond distance for the water molecule

Table S3: Summary of x-ray and neutron diffraction data for crystalline amino acid monohydrates.

Sample	Crystal System	Space Group	a (Å)	b (Å)	c (Å)	Source
Arg	Monoclinic	$P2_1$	11.049	8.487	11.226	x-ray[5]
Asn	Orthorhombic	$P2_12_12_1$	5.593 5.580	9.827 9.743	11.808 11.706	neutron[6] x-ray[7]
Asp	Orthorhombic	$P2_12_12_1$	5.587	9.822	11.83	neutron[8]
Cys	Orthorhombic	$P2_12_12_1$	5.458	7.157	19.389	x-ray[9]
Gly-Gly	Monoclinic	$P2_{1/c}$	8.813 8.813	9.755 9.755	9.788 9.788	x-ray[10] neutron[11]
Gly-Gln	Orthorhombic	$P2_12_12_1$	5.415	11.618	15.558	x-ray[12]
His	Orthorhombic	$P2_12_12_1$	15.301 15.36	8.921 8.92	6.846 6.88	x-ray[13] neutron[14]

References:

1. Gervais, C.; Dupree, R.; Pike, K. J.; Bonhomme, C.; Profeta, M.; Pickard, C. J.; Mauri, F., Combined First-Principles Computational and Experimental Multinuclear Solid-State NMR Investigation of Amino Acids. *The Journal of Physical Chemistry A* **2005,** *109* (31), 6960-6969.

2. Lemaitre, V.; Smith, M. E.; Watts, A., A Review of Oxygen-17 Solid-State NMR of Organic Materials - Towards Biological Applications. *Solid State Nuclear Magnetic Resonance* **2004,** *26* (3-4), 215-235.

3. Pike, K. J.; Lemaitre, V.; Kukol, A.; Anupold, T.; Samoson, A.; Howes, A. P.; Watts, A.; Smith, M. E.; Dupree, R., Solid-State ^{17}O NMR of Amino Acids. *Journal of Physical Chemistry B* **2004,** *108* (26), 9256-9263.

4. Wong, A.; Howes, A. P.; Yates, J. R.; Watts, A.; Anupold, T.; Past, J.; Samoson, A.; Dupree, R.; Smith, M. E., Ultra-High Resolution ^{17}O Solid-State NMR Spectroscopy of Biomolecules: A Comprehensive Spectral Analysis of Monosodium L-Glutamate Monohydrate. *Physical Chemistry Chemical Physics* **2011,** *13*, 12213-12224.

5. Xian, L.; Lu, G.-X., L-Arginine Hydrochloride Monohydrate. *Chemical Research and Application* **2007,** *19*, 474.

6. Ramanadham, M.; Sikka, S. K.; Chidambaram, R., Structure of L-Asparagine Monohydrate by Neutron Diffraction. *Acta Crystallographica* **1972,** *B28*, 3000-3005.

7. Flaig, R.; Koritsanszky, T.; Dittrich, B.; Wagner, A.; Luger, P., Intra- and Intermolecular Topological Properties of Amino Acids: A Comparative Study of Experimental and Theoretical Results. *Journal of the American Chemical Society* **2002,** *124*, 3407-3417.

8. Umadevi, K.; Anitha, K.; Sridhar, B.; Srinivasan, N.; R.K., R., L-Aspartic Acid Monohydrate. *Acta Crystallographica* **2003,** *E59*, 01073-01075.

9. Chapman, R. P.; Bryce, D. L., A High-Field Solid-State Cl-35/37 NMR and Quantum Chemical Investigation of the Chlorine Quadrupolar and Chemical Shift Tensors in Amino Acid Hydrochlorides. *Physical Chemistry Chemical Physics* **2007,** *9* (47), 6219-6230.

10. Parthasarathy, R., Crystal Structure of Glycylglycine Hydrochloride. *Acta Crystallographica* **1969,** *B25*, 509-518.

11. Koetzle, T. F.; Hamilton, W. C.; Parthasarathy, R., Precision Neutron Diffraction Structure Determination of Protein and Nucleic Acid Components. II. The Crystal and Molecular Structure of the Dipeptide Glycylglycine Monohydrochloride Monohydrate. *Acta Crystallographica* **1972,** *B28*, 2083-2090.

12. Panneerselvam, K.; Soriano-Garcia, M., L-Glycyl-L-Glutamine Monohydrate. *Acta Crystallographica* **1995,** *C51* (12), 2718-2720.

13. Oda, K.; Koyama, H., Refinement of Crystal-Structure of Histidine Hydrochloride Monohydrate. *Acta Crystallographica* **1972,** *B28*, 639-642.

14. Fuess, H.; Hohlwein, D.; Mason, S. A., Neutron Diffraction Study of L-Histidine Hydrochloride Monohydrate. *Acta Crystallographica* **1977,** *B33*, 654-659.